18TH WORLD CONFERENCE ON EARTHQUAKE ENGINEERING
WCEE2024
MILAN

MILAN, ITALY
30TH JUNE - 5TH JULY 2024

www.wcee2024.it

INTERIOR BEAM-COLUMN CONNECTIONS WITH DIFFERENT STRENGTH RATIO AND JOINT HOOP REINFORCEMENT RATIO

N. Onishi[1], S. Tajiri[1] & H. Shiohara[1]

[1] The University of Tokyo, Tokyo, Japan, onishi@arch1.t.u-tokyo.ac.jp

Abstract: *Beam-column joints in reinforced concrete frame structures must minimize deformation without failure to ensure that the system has the seismic performance expected at the design stage, even when stresses due to a strong earthquake act on the beam-column joint. Specifically, the end of beam longitudinal bars yield rather than the longitudinal bars in the beam-column joint, and the beam must show stable flexural behavior even under severe deformation conditions. The column-to-beam strength and joint transverse reinforcement ratios are crucial factors in controlling performance.*

This paper investigates the effects of the column-to-beam strength ratio and the joint transverse reinforcement ratio on joint behavior by testing six interior beam-column joint specimens. The high column-to-beam strength ratio and joint transverse reinforcement ratio mitigated the pinching in hysteresis. Although the joint hoops yielding during large deformation was not wholly suppressed, distinct beam yield hinges formed in a specimen with a column-to-beam strength ratio of 1.88 and a joint transverse reinforcement ratio of 1.1 percent.

Finite element analyses were conducted to examine the experimental results. Although the analysis showed little difference in pinching behavior between the specimens with different joint transverse reinforcement ratios, the deformation of the columns, beams, and a joint were close to that in the experiment, at least until up to a 2% drift cycle.

1. Introduction

For a reinforced concrete frame structure to have the seismic performance expected at the time of design, it has to meet the following conditions: the beam's ultimate strength must be reached without significant reduction in stiffness up to beam yielding, even if large earthquake stress acts on the beam-column connection; a distinct yield hinge must form at the end of the beam, with which the strength maintains after the beam reaches its ultimate strength; the concrete and reinforcing bars of the joint panel must stay within their elastic range; and hold stably the axial loads acting from the columns, and the frame must form a beam mechanism even if the story drift increases so that there is no concentration of deformation in a particular story. It is considered that the joints should have sufficient column-to-beam strength ratios and joint transverse reinforcement ratios to achieve these performances.

The authors, therefore, carried out experiments on six interior (cruciform) beam-column joint specimens, in which the two parameters were the column-to-beam strength ratio and the joint transverse reinforcement ratio (Onishi et al., 2019). In this paper, the effects of the column-to-beam strength ratio and the amount of transverse reinforcement at the joint on the behavior of the joints are discussed, and finite element analyses are performed on two specimens to compare to the experimental results.

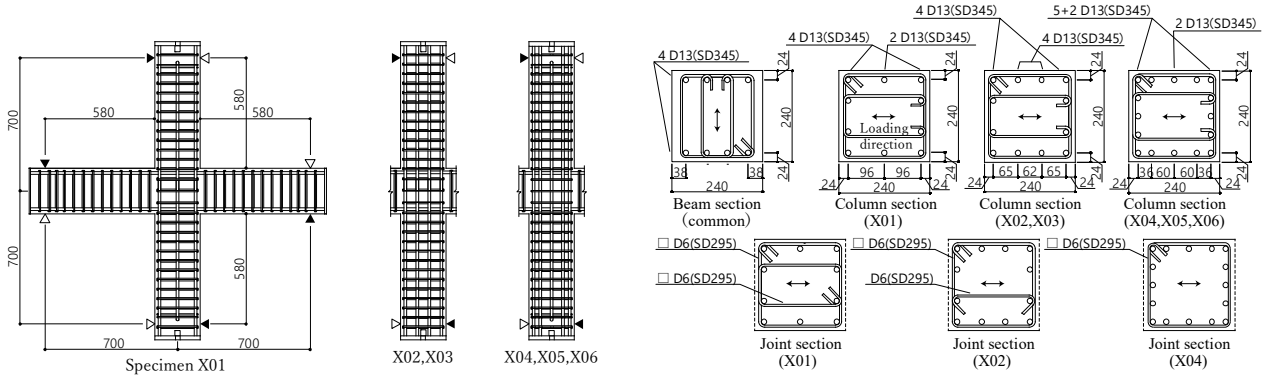

Figure 1. Details of specimens.

Table 1. Test parameters.

Column-to-beam strength ratio ΣMcu′/ΣMbu′	Joint reinforcement factor Ajfjy/Atfy		
	0.46	**0.70**	**0.93**
1.24			**X01**
1.47		**X02**	**X03**
1.88	**X04**	**X05**	**X06**

Table 2. Specimen specifications

	Name	X01	X02	X03	X04	X05	X06
COLUMN	Longitudinal bars	10 D13	12 D13		16 D13		
		SD345					
	Reinforcement ratio p_g	2.20%	2.64%		3.52%		
	Transverse reinforcement	4 D6(SD295A)@50 mm Transverse reinforcement ratio: 1.06%					
BEAM	Tensile reinforcement	4 D13(SD345) Tensile reinforcement ratio: 0.98%					
	Transverse reinforcement	4 D6(SD295A)@50 Transverse reinforcement ratio: 1.06%					
JOINT	Joint transverse reinforcement	▥ D6 (3 sets)	◫ D6 (3 sets)	▥ D6 (3 sets)	□ D6 (3 sets)	◫ D6 (3 sets)	▥ D6 (3 sets)
	Reinforcement ratio of joint	1.10%	0.82%	1.10%	0.55%	0.82%	1.10%
Column-to-beam strength ratio*1		1.24	1.47		1.88		
Joint reinforcing factor*2		0.93	0.70	0.93	0.46	0.70	0.93
Strength deteriorating factor β_j		1.20	1.27	1.32	1.44	1.48	1.53

*1 Ratio of column-to-beam moment strength at joint.
*2 Ratio of the product of total cross-sectional area and yield strength of the joint hoops to the tensile yield force of the beam longitudinal reinforcement.

Table 3. Material properties of steel

Use	Diameter (Nominal strength)	Yield strength (MPa)	Young's modulus (GPa)	Tensile strength (MPa)
Longitudinal bars	D13 (SD345)	374	184	508
Transverse bars	D6 (SD295A)	347*	194	497

*0.2% offset yield strength.

Table 4. Material properties of concrete

Compressive strength (MPa)	Young's modulus (GPa)	Strain at compressive strength (10^{-6} m/m)	Tensile splitting strength (MPa)
36.8	28.6	2189	2.49

2. Experiment of interior beam-column joint specimen

2.1. Experimental methods

Test specimens

Six 1/3-scale interior beam-column joint specimens were fabricated with two experimental variables: the column-to-beam strength ratio and the amount of transverse reinforcement at the joint. Table 1 shows the relationship between the specimen names and the test variables. Figure 1 shows the rebar arrangement, and Table 2 shows the specimen specifications. Tables 3 and 4 show the material property values of the rebar and concrete (at the time of the experiment) obtained from the material tests. The values shown as concrete strength are the average of the material tests during the test period. The calculated values in Table 2 were obtained using the values in Tables 3 and 4.

Shear reinforcement bars were placed at 50 mm pitch from 25 mm away from the column face for the beams and from the column face for the columns. The shear reinforcement ratio of columns and beams was set at

approximately 1% to prevent deterioration of the bearing capacity due to damage to the concrete at the ends of members after flexural yielding.

The column-to-beam strength ratio of X01 was 1.24, X02 and X03 were 1.47, and X04 through X06 were 1.88. The joint reinforcing factor, defined as the ratio of the product of the total cross-sectional area and yield strength of the transverse reinforcement at the joint to the tensile force at yield of the beam longitudinal bars, was 0.46 (0.55%) for X04, 0.70 (0.82%) for X02 and X05, and 0.93 (1.10%) for X01, X03, and X06 (the values in parentheses are joint transverse reinforcement ratio). Table 2 also shows the strength deteriorating factor due to beam-column joint yielding, βj, as shown in the "beam-column joints" clause of the AIJ (2021). This value is an indicator of whether the strength at yielding of the joint is sufficient for the beam bending strength, and it is recommended in the commentary that the value should be 1.5 or more. Of the six specimens tested, only X06 satisfied this criterion.

Loading and measurement

The experiments were conducted using the same loading method used in the previous experiments (Kusuhara et al., 2010), as shown in Figure 2. The force was transferred to the specimen by applying the force horizontally to the loading beam with an oil jack. The high-strength steel rods were tethered to the loading frame via spherical washers to zero bending moments at the points of contraflexure of the columns and beams. Since the columns do not support the specimen vertically, the weight of the specimen is applied to the high-strength steel rods of both beams. Loads were measured by load cells installed on the end of the loading frame side of the horizontal high-strength steel rods connected to the columns' contraflexure points. The drift ratio was obtained by dividing the sum of the average displacements of the laser displacement transducers, two each on the upper and lower columns, by the distance between the upper and lower points of contraflexure of the columns (1400 mm).

Figure 3 shows the loading history. The force was applied until about half of the crack strength was reached in the first cycle, and after that, the displacement control was applied by alternating loading with the target drift ratios of ±0.25%, ±0.5%, ±1.0%, ±1.5%, and ±2.0%, increasing by 1% up to 5% for X01, 7% for X02 through X05, and 8% for X06. One alternating loading cycle was added at each drift cycle of 1% and after.

Two strain gauges were applied to the longitudinal bars of the columns and beams, one facing each other at the intersection, and two strain gauges were applied to the three transverse reinforcement bars at the joints, excluding the tie bars, facing each other in the middle of the column depth.

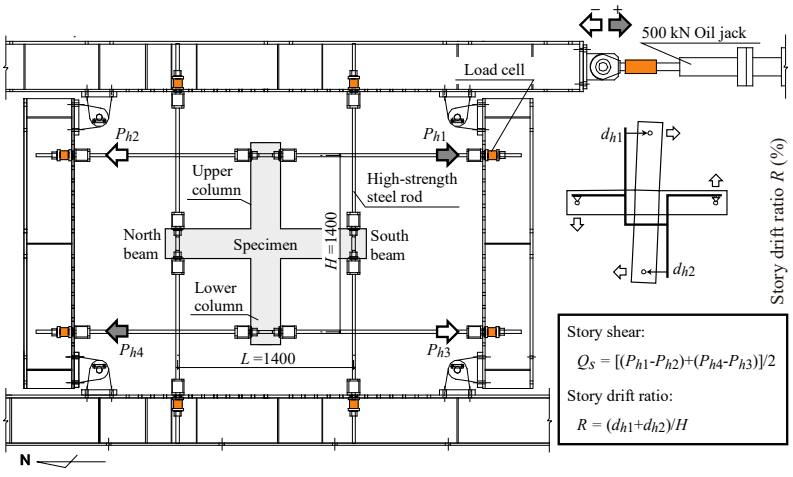

Figure 2. Loading setup

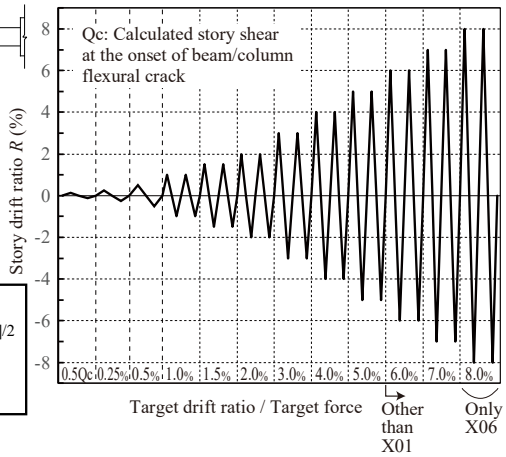

Figure 3. Loading history

2.2. Experimental results

Failure process of specimens and yielding of rebars

Figure 4 shows the area around the joint at the peak of the second −4% drift cycle, and Table 5 lists the characteristic points obtained from the experiments. In all specimens, the cracks first appeared diagonally from the joint panel's inside corner toward the joint's center. Then, these cracks propagated along the column

longitudinal bars from near the intersection of the longitudinal bars of the columns and beams. Diagonal cracks were observed at the center of the joint, and these diagonal cracks closed, and orthogonal cracks appeared when the load was applied in the opposite direction. Flexural cracks at the top and bottom of beam ends were connected during a 1% drift cycle.

X01, X03, and X06, with a transverse reinforcement ratio of 0.93, are compared. The strain in the joint transverse reinforcement of X01 reached the yield strain before the beam bars yielded, and the diagonal cracks at the joint were wider than the flexural crack at the beam ends after the beam bars yielded. On the other hand, the damage to the joint panel concrete of X06 was less severe, and the flexural cracks at the beam ends were larger than those of X01. The diagonal cracks at the joint of X03 were wider than those of X06, but the flexural cracks were relatively wider. Next, X04 to X06 with a column-to-beam strength ratio of 1.88 are compared. The specimens with higher joint transverse reinforcement ratios showed less damage to the concrete at the joints.

The beam reinforcement yielded during the 1% drift cycle, except for X01, whose beam reinforcement yielded at a drift ratio of +1.07% during the 1.5% drift cycle. The specimens with a higher column-to-beam strength ratio showed less strain in the first layer of the column tensile longitudinal bars.

The X01 specimens yielded during the first 1.5% drift cycle, and the others yielded during the first 1% drift cycle. Increased strain in the joint transverse reinforcement was observed up to a 4% drift ratio. Comparing specimens with the same column-to-beam strength ratio, the specimens with a higher joint reinforcing factor showed less strain in the joint transverse reinforcement.

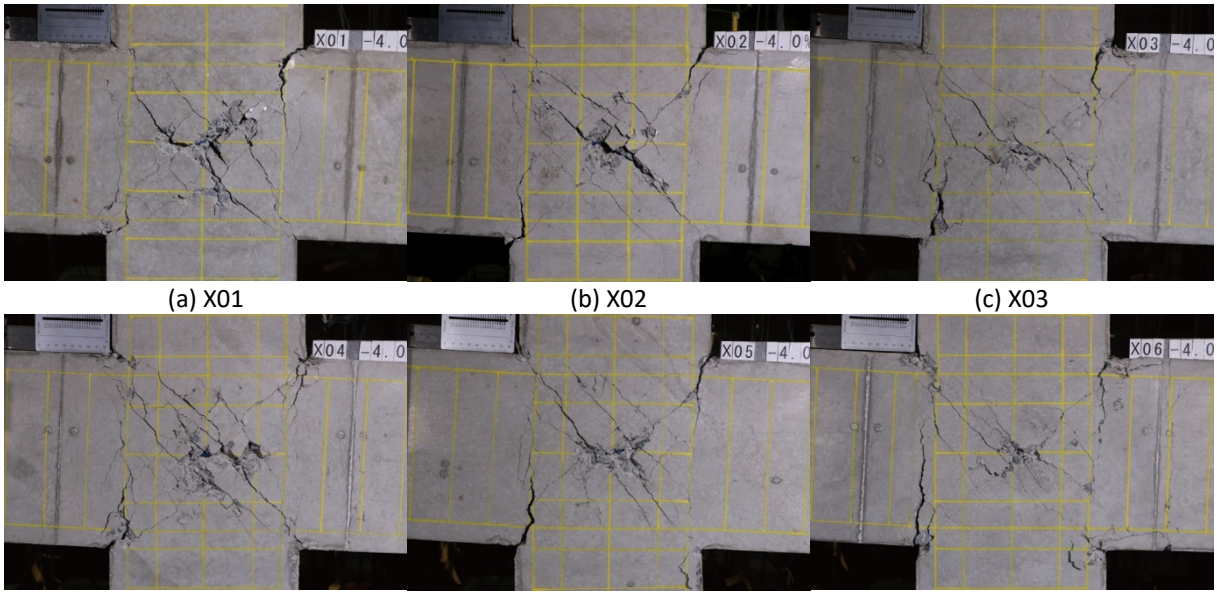

(a) X01 (b) X02 (c) X03

(d) X04 (e) X05 (f) X06

Figure 4. Failure conditions at the peak of the second −4% drift cycle.

Story shear–drift ratio relationship

Figure 5 shows the relationship between story shear force and story drift ratio. The figure also shows the yielding of the column longitudinal bar (cy) and the beam longitudinal bar (by); the yielding of the middle set of joint hoops (jy); the maximum story shear force (▽); and the calculated story shear at beam's ultimate strength (dashed line). In the beam's ultimate strength calculations, modified Kent-Park was applied to the concrete, and a bilinear model was assumed for the steel bars. Material test values in Tables 3 and 4 were applied for material properties.

The maximum shear force generally exceeded the calculated values, and the difference between specimens was slight. All specimens showed pinching in hysteresis. However, the specimens with a larger column-to-beam strength ratio and those with a higher joint reinforcing factor had a larger difference between the maximum and minimum load values at 0% drift ratio, i.e., the degree of pinching of the hysteresis loops was smaller.

Table 5. Characteristic points from the experiment.

Name of specimen		X01	X02	X03	X04	X05	X06
Initial stiffness (kN/mm)		25.3	19.7	22.6	26.2	18.0	17.3
First crack at the inside corner of joint panel (kN)	+	11.3	8.6	8.3	7.5	7.3	5.7
	−	−4.4	−6.6	−5.5	−5.4	−4.3	−4.6
First diagonal crack in the middle of the joint (kN)	+	21.1	18.6	17.0	18.0	22.9	20.5
	−	−14.0	−19.1	−21.9	−18.0	−19.8	−18.8
Yield of beam longitudinal reinforcement (kN)	+	60.6 (1.07)	56.1 (0.91)	57.0 (0.88)	57.9 (0.87)	56.6 (0.78)	58.8 (0.88)
	−	−57.8 (−0.97)	−56.4 (−0.90)	−59.9 (−0.94)	−53.6 (−0.76)	−53.2 (−0.77)	−54.2 (−0.80)
Yield of first-layer column longitudinal reinforcement (kN)	+	62.2 (1.12)	66.7 (1.31)	60.2 (1.45)	58.7 (4.32)	68.5 (4.92)	68.3 (5.01)
	−	−54.6 (−1.02)	−65.6 (−1.47)	−60.3 (−1.56)	−59.5 (−4.70)	−66.7 (−3.85)	No yielding
Yield of middle-layer joint hoop (kN)		66.6 (1.33)	49.3 (0.77)	52.7 (0.79)	53.3 (0.78)	55.3 (0.76)	62.0 (0.94)
Maximum shear force (kN)	+	70.8 (2.86)	71.0 (2.95)	73.2 (2.92)	72.2 (3.00)	73.8 (2.89)	72.3 (2.99)
	−	−65.4 (−2.95)	−68.7 (−2.98)	−69.4 (−3.98)	−67.2 (−2.87)	−69.0 (−2.88)	−69.0 (−2.94)

* Numbers in parenthesis are drift ratio (%) at the load in the first line of each cell.

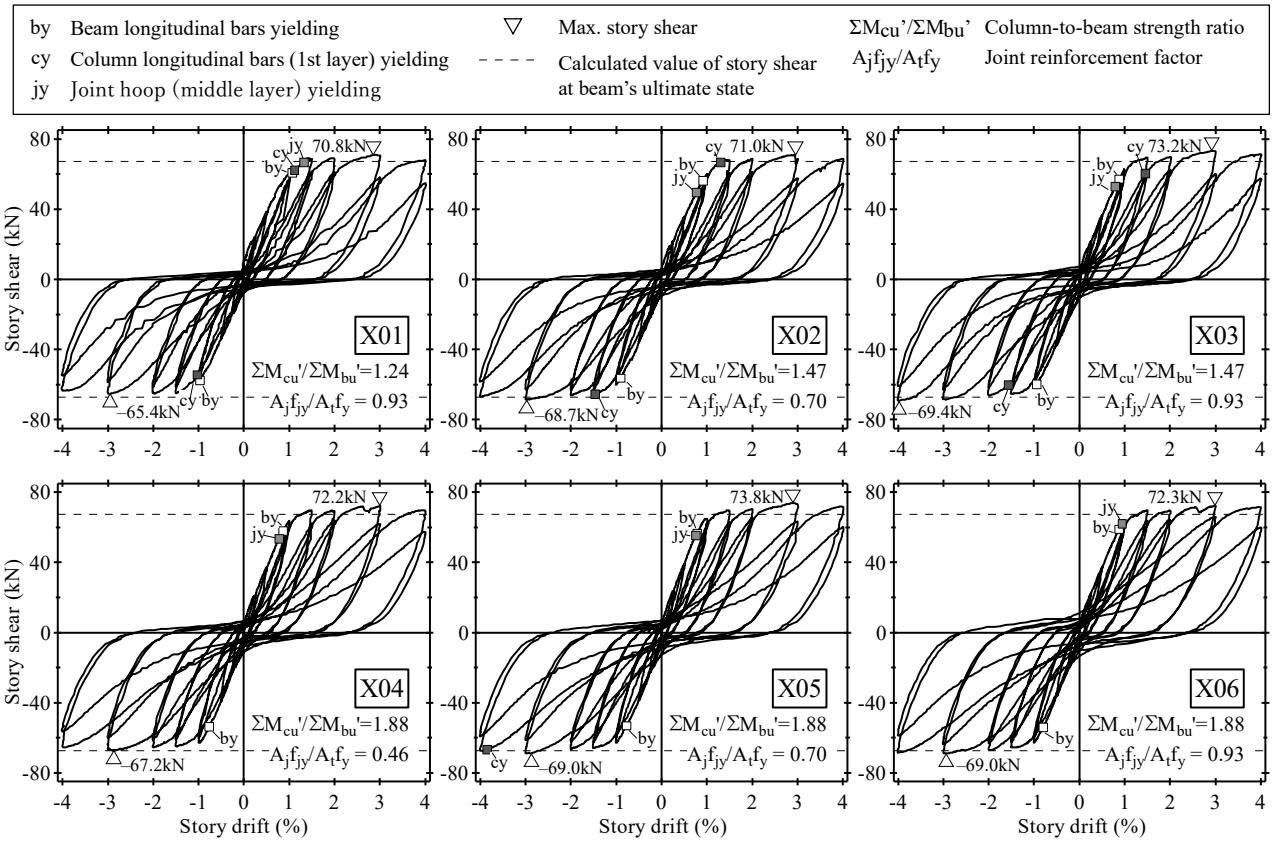

Figure 5. Story shear–story drift ratio relationship.

Deformation ratio of components

Figure 6 shows the equivalent drift ratio of columns, beams, and joint panels converted from each deformation to story drift ratio. The chord rotations, member end rotations, and joint deformations were obtained using the previous method (Kusuhara et al., 2006). The drift ratios of the columns and beams contain deflection and member end rotation, while the drift ratio of the joint contains joint rotation and joint shear deformation. The specimens with larger joint transverse reinforcement ratios tended to have less joint deformation. The beam's deformation of X06 accounted for about 70% of the total deformation, even at a drift ratio of 4%. Figure 4 also showed that X06 formed clear yield hinges at the beam ends.

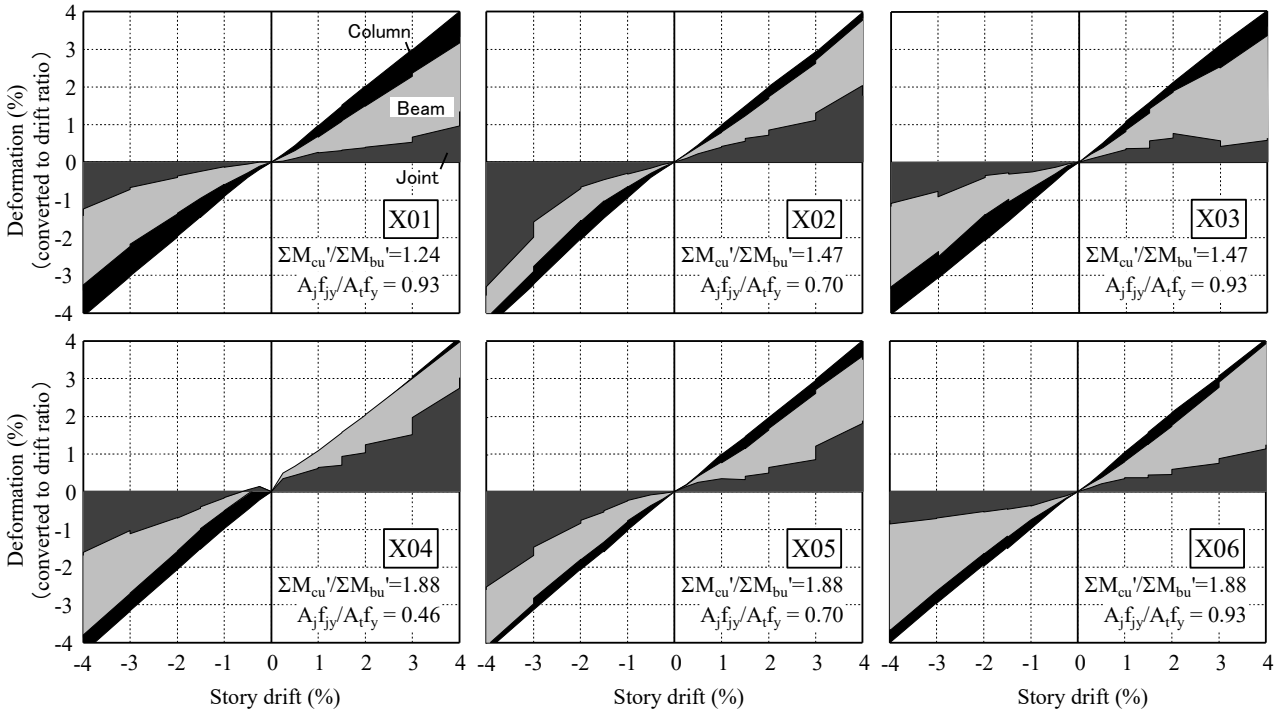

Figure 6. Deformation of each component converted to drift ratio.

2.3. Discussion

Effect of column-to-beam strength ratio

This section compares specimens with the same joint reinforcing factor. X06, with a higher column-to-beam strength ratio, showed less cracking and spalling of the cover concrete than X01, with a lower strength ratio. X01 also showed flexural cracks at the beam ends. However, they were located along the column longitudinal reinforcement inside the column face, and the deformation ratio of the beam was not as large as that of X06. Damage on the joint of X03 was almost the same as X06 in the drift ratio of up to 4%.

Similarly, comparing X02 and X05 in Figure 4, X05 appears to have slightly less joint damage; there is little difference in the joint deformation between X02 and X05 during the positive loading, while during the negative loading, the joint deformation of X02 increased from about 3–4% drift cycle, indicating that the joint damage was more significant than that of X05. The deformation ratio of the columns and joints tended to be smaller for the specimen having the higher column-to-beam strength ratio. However, the extent of the tendency depended on the joint reinforcing factor. X03, with a high joint reinforcing factor, showed less damage at the joints and a larger deformation at the beams, even though the column-to-beam strength ratio was about 1.5.

Effect of joint hoop reinforcement ratio

This section compares two specimens with the same column-to-beam strength ratio. Comparing X04 and X06 in Figure 4, X06, with a higher joint reinforcing factor, has less cracking and spalling of the cover concrete at the joint. The transverse reinforcement ratio of the joint of X06 was 1.1%, which was twice as much as X04. As the yielding of joint hoops of X06 occurred at a larger drift than X04, the joint hoops may have reduced the damage to the joints. Similarly, X03 had less joint damage than X02. It was confirmed that the joint hoops effectively reduced the damage at the joint regardless of the column-to-beam strength ratio. However, yielding of the middle joint hoop was observed at a drift ratio of 1–1.5% for all specimens.

3. Finite element analyses

Finite element analysis was used to visualize the stress field in the concrete of the specimens. The target specimens were X04 and X06, with a column-to-beam strength ratio of 1.88 and a different joint reinforcing factor. Onishi et al. (2023) showed that it is difficult to match the deformation of each part to the experimental results as the deformation increases. Therefore, this study analyzed the specimens in smaller element sizes for the beam and column ends around the joints.

3.1. Settings of analysis models

Figure 7 shows the analytical model. The model consisted of only half of the specimen, using the symmetry in width. Elements near the supports and the contraflexure points were linear elastic elements with sufficiently high stiffness. In the analysis, the values in Table 3 were used for the compressive strength, tensile strength, and Young's modulus of concrete, and the values in Table 4 were used for the yield strength and Young's modulus of steel bars. The strain at the maximum strength of the concrete was constant at 0.002 m/m. X04 and X06 differ in the joint reinforcing factor.

The nonlinear finite element analysis program FINAL(V11) (Obayashi Corporation) was used for the analysis. Eight-node hexahedron elements were used for the concrete, line elements for the reinforcement, and spring elements ("line element") between the concrete nodes and reinforcement nodes to give the relationship between the bond stress and the slip displacement. The bond strength was given in accordance with the AIJ (1999), and the slip displacement at the bond strength was set to 1.0 mm with reference to the case of "good bond conditions" in FIB (2013). Table 6 summarizes the material models used in the analysis.

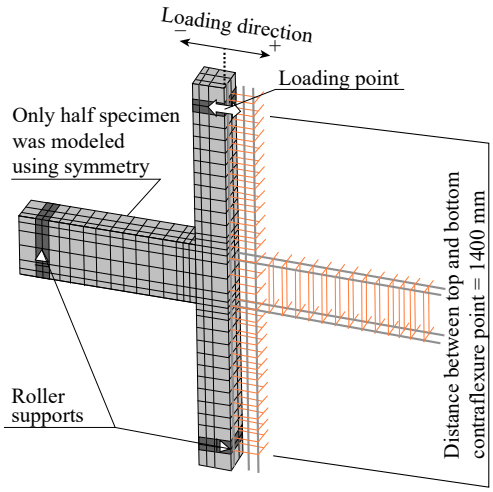

Figure 7. Analytical model.

Table 6. Material models used in the analysis.

Concrete	Tension stiffening	Izumo et al. (1987) (coefficient C=1.0)
	Stress–strain curve under compression	Modified Ahmad model (Naganuma, 1995)
	Compression failure condition	Ottosen four-parameter model with Hatanaka's factor (Naganuma, 1995)
	Softening characteristics under compression	Nakamura and Higai (1999)
	Hysteresis model under cyclic loading	Naganuma and Okubo (2000)
	Shear transfer model for concrete with cracks	Naganuma (1991)
Steel	Hysteresis model	Bilinear
	Strain hardening	Isotropic hardening law
Bond	Bond stress–slip curve	Naganuma et al. (2004)

3.2. Analysis results

Story shear–story drift ratio relationships

Figure 8 shows the relationship between story shear force and story drift ratio. Compared to the experiment, the shear force of the analysis slightly overestimated that of the experiment, and the unloading stiffness was relatively low. In the experiment, cracks create gaps in the concrete, and when unloading occurs, the rebar in that area releases elastic strain first, resulting in high stiffness at unloading. This is why the unloading stiffness in the analysis was lower than in the experiment. Additionally, the pinching behavior in the experiment tended to be slightly stronger in X04, but the analysis showed little difference in the outline of hysteresis loops between X04 and X06.

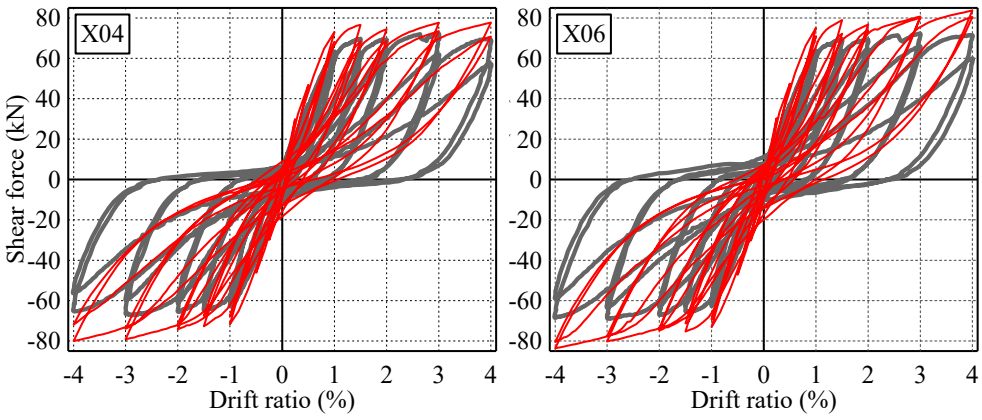

Figure 8. Story shear–story drift ratio relationship.

Deformation ratio of components

Figure 9 shows the deformation of the columns, beams, and a joint of X04 and X06, with the deformation converted to drift ratio on the horizontal axis and the story shear force on the vertical axis. The drift ratio of the beams of the X04 case was generally close to the experiment. However, in the X06 case, the drift ratio of the beams did not reach the experimental value after the 2% drift cycle. To match the experimental results, minimizing the element size at the ends of the beams may be necessary, where plastic deformation was large in the experiment.

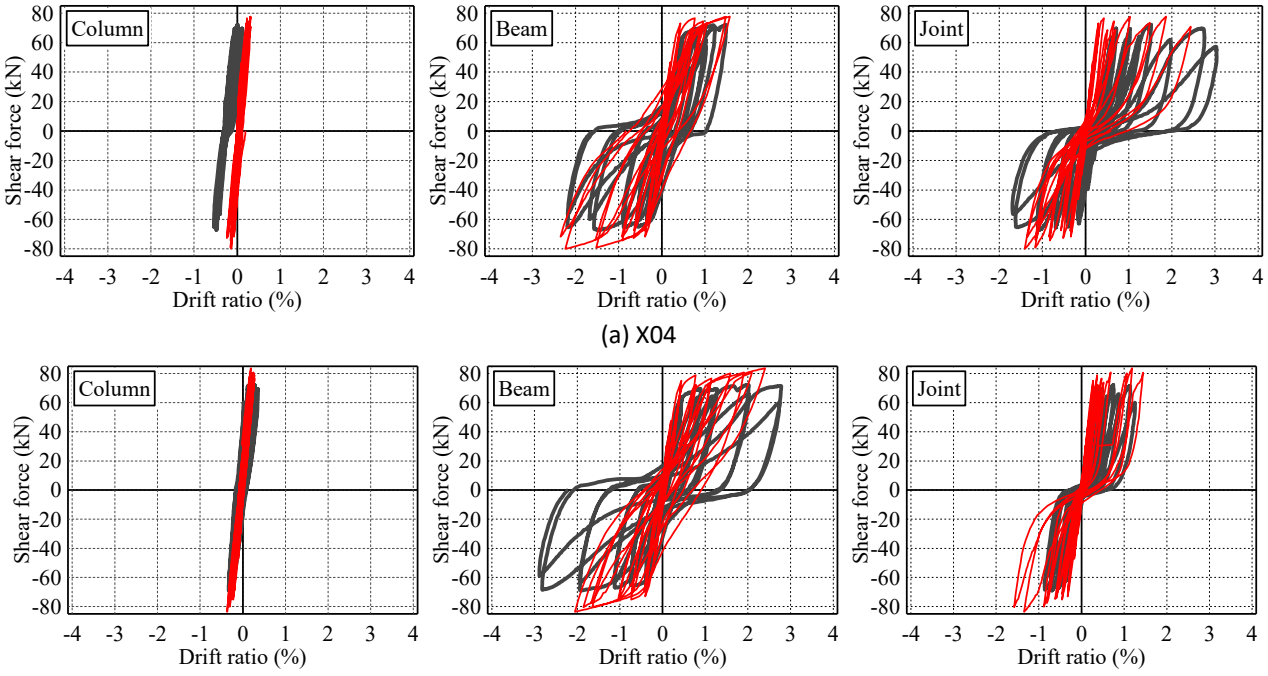

(a) X04

(b) X06

Figure 9. Deformation of each component converted to drift ratio.

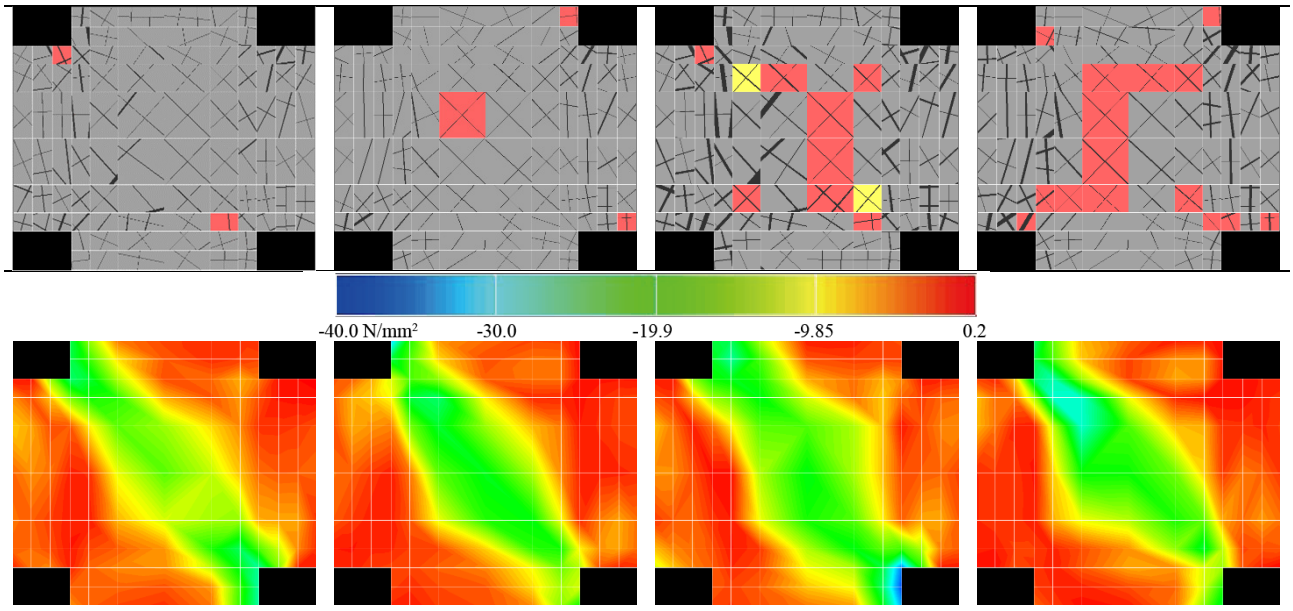

(a) X04 (b) X06 (c) X04 (d) X06

Figure 10. Crack pattern diagram and minimum principal stress contour plot.

Cracks and softening of concrete

Figure 10 shows the surface crack diagrams and the minimum principal stress diagrams of the center-in-width cross section at the peak drift of the first cycle of −2% and −4% drift cycle. Comparing the crack diagrams, the cracks in the joint panel concrete were slightly more noticeable in X04, which has a lower joint reinforcing factor. However, there was no difference among the specimens in the number of softening elements (red and yellow elements in the figure). There was a distinct diagonal compression strut in the minimum principal stress contour diagram when the drift ratio was small, but as the drift ratio increased, the contour of the strut widened, and the maximum value of the existent stress decreased. There was no significant difference between X04 and X06 cases. However, considering the overestimation of the drift ratio of the X06 joint after the 2% drift ratio, the X06 joints may have less damage if the model is modified. Further discussion is required.

4. Conclusions

The effects of the column-to-beam strength ratio and the amount of joint transverse reinforcement on the behavior of the beam-column connections were investigated by testing six interior beam-column joint specimens. Finite element analyses were also conducted to visualize the stress field of the concrete in the experiments.

The findings from the experiments are as follows:

1. The relationship between story shear force and story drift ratio did not affect the maximum strength. All the specimens showed pinching hysteresis loops, and the higher the column-to-beam strength ratio or the joint reinforcing factor, the larger the difference between the maximum and minimum values of the load at 0% drift ratio, and the weaker the pinching.
2. The deformations of the columns and joint tended to decrease with increasing the column-to-beam strength ratio, but the extent of the decrease depended on the joint reinforcing factor. For X03, having the highest joint transverse reinforcement ratio, damage at the joint was reduced, and the deformation of the beams was relatively large, even though the column-to-beam strength ratio was approximately 1.5.
3. Joint transverse reinforcement reduced the damage at the joint regardless of the column-to-beam strength ratio. However, all specimens yielded the middle set of joint hoops during a 1–1.5% drift cycle.

The following findings were also obtained from analyzed X04 and X06, having different joint reinforcing factors.

4. The relationship between story shear force and story drift ratio was close to the experiment, although the maximum shear force was slightly overestimated, and the unloading stiffness was lower than in the experiment. The pinching behavior was also observed in the analysis, but there were few differences in the analyses with different joint reinforcing factors.
5. The deformation of the columns, beams, and a joint of X04 was close to that in the experiment, even at a drift ratio of 4%. However, the deformation of the components of X06 was similar to that in the experiment until up to 2%, but after 2%, the beam deformation was not as large as in the experiment.
6. In the crack pattern diagrams, cracks in the joint concrete were slightly more significant for X04, which has a smaller joint reinforcing factor. There was no significant difference in the number of softened elements. The minimum principal stress contour diagram also showed little difference between X04 and X06. However, this result could be changed by adjusting the analytical model of X06 to match the deformation of each component to the experiment.

Acknowledgment

This work was supported by JSPS KAKENHI Grant Number JP16H04446 (PI: Hitoshi Shiohara).

References

AIJ (1999). *Design Guideline for Earthquake Resistant Reinforced Concrete Buildings Based on Inelastic Displacement Concept*, Architectural Institute of Japan, Tokyo. (in Japanese)

AIJ (2021). *AIJ Standard for Lateral Load-carrying Capacity Calculation of Reinforced Concrete Structures*, Architectural Institute of Japan, Tokyo. (in Japanese)

FIB (2013). *fib Model Code for Concrete Structures 2010*, Federation Internationale du Beton, Lausanne.

Izumo J., Shima H., Okamura H. (1987). Analytical model for reinforced concrete panels under in-plane stresses, *Concrete Journal*, 25(9): 107–120. (in Japanese)

Kusuhara F, Shiohara H. (2006). Deformation, stress, and measurement method of RC beam-column joint subassemblages including joint rotation, *Proceedings of the Japan Concrete Institute*, 28(2): 355–360. (in Japanese)

Kusuhara F., Shiohara H., Tazaki W., Park S. (2010). Seismic performance of reinforced concrete interior beam-column joint under low ratio of column to beam moment capacity, *Transactions of AIJ. Journal of Structural and construction engineering*, 75(656): 1873–1882. (in Japanese)

Naganuma K. (1991). Nonlinear analytical model for reinforced concrete panels under in-plane stresses, Study on nonlinear analytical method for reinforced concrete wall structures (Part 1), *Transactions of AIJ. Journal of Structural and construction engineering*, 421: 39–48. (in Japanese)

Naganuma K. (1995). Stress-strain relationship for concrete under triaxial compression, *Transactions of AIJ. Journal of Structural and construction engineering*, 60(474): 163–170. (in Japanese)

Naganuma K., Okubo M. (2000). An analytical model for reinforced concrete panels under cyclic stresses, *Transactions of AIJ. Journal of Structural and construction engineering*, 536: 135–142. (in Japanese)

Naganuma K., Yonezawa K., Kurimoto O., Eto H. (2004). Simulation of nonlinear dynamic response of reinforced concrete scaled model using three-dimensional finite element method, *Proceedings of the 13th World Conference on Earthquake Engineering*, Paper No. 586.

Nakamura H., Higai T. (1999). Compressive fracture energy and fracture zone length of concrete, modeling of inelastic behavior of RC structures under seismic loads, *ASCE*, 627(44): 471–487.

Obayashi Corporation. FINAL. Available at: https://www.obayashi.co.jp/solution_technology/detail/tech_d061.html (Accessed: 4 October 2023). (in Japanese)

Onishi N., Shiohara H. (2021). Experimental study on effects of joint hoops for failure mechanism of reinforced concrete interior beam-column joint, *Proceedings of the Japan Concrete Institute*, 41(2): 319–324. (in Japanese)

Onishi N., Tajiri S., Shiohara H. (2023). Finite element analysis with concrete strength parameter of RC interior beam-column connections formed yield hinge, *Proceedings of the Japan Concrete Institute*, 45(2): 439–444. (in Japanese)